Geomechanics and Engineering, *Vol. 26, No. 4 (2021) 345-355*
https://doi.org/10.12989/gae.2021.26.4.345

Compression behavior of cement-treated marine dredged clay in Dalian Bay

Jianwen Ding[a], Xing Wan*, Jianhua Wang, Cong Mou and Mengying Gao

Department of Underground Engineering, Southeast University, NO.2 Southeast University Road, Jiangning District, Nanjing, China

(Received March 11, 2021, Revised May 31, 2021, Accepted August 4, 2021)

Abstract. There exists large volume of marine dredged clay generated worldwide to potentially compromise to ocean environment. Efficient resource utilization of dredged clay is crucial to sustainable development of offshore works. In this study, cement-treated marine dredged clay is suggested as filling materials for the construction of artificial islands in Dalian Bay, China. To evaluate influence of cement addition on compressibility, a series of oedometer tests were performed on reconstituted and cement-treated dredged clay. The effects of initial water content, cement content and curing time were examined. In addition, the pore fluid salinity effect on reconstituted and cemented dredged clay was explored by desalination treatment, respectively. The testing results show that the vertical yield stress of cemented dredged clay is governed by initial water content while the compressibility in post-yield state is determined by cement content. The influence of curing time is more significant for the specimens with higher initial water content. The compressibility of reconstituted dredged clay decreases when increasing salinity of pore fluid, but pore salt accelerates the degradation of artificial structure of cemented clay. Moreover, a practical predicting method was presented based on the experimental data. Both the pre-yield compression index C_s and post-yield compression index C_c are correlated with the yielding point. The proposed method enables to more quickly capture the compression curves of cement-treated dredged clay in practice.

Keywords: cement-treated; compression behavior; marine dredged clay; pore fluid salinity; predicting method

1. Introduction

Large volume of dredged clay, generated from harbor construction and waterway maintenance, is often featured by high water content and clay content, which leads to the undesirable engineering characteristics (e.g., high compressibility, low strength and permeability). (Kim *et al.* 2015, Yoobanpot *et al.* 2018, Slimanou *et al.* 2020, Yamashita *et al.* 2020). It is reported that nearly 150 million cubic meters of dredged clay is discarded into ocean in China, posing a great threat to marine environment (Xu *et al.* 2020), Recently, traditional disposal methods of dredged materials are gradually abandoned and prohibited for protection of marine environment, and more attention is thus paid to environmental friendly resource utilization of dredged clay (Çevikbilen *et al.* 2020).

Solidification technology can be adopted to convert semi-solid dredged materials into monolithic solids. Using solidified materials as land reclamation, road pavement and dike filling is thus an effective solution to solve the problem previously mentioned. Zhang *et al.* (2007) first reported a large-scale engineering application in China, where approximately 1.8×10^6 m^3 of dredged materials from Taihu Lake were effectively handled. Ordinary Portland cement has been the most popular binder used in solidification technology worldwide. Meanwhile, some other cost-effective and environmental-friendly materials [e.g., fly ash, lime and phosphogypsum] are also advantageous for the soil stabilization (Ding *et al.* 2019b, Arefnia *et al.* 2020, Mymrin *et al.* 2021, Vafaei *et al.* 2021). However, they are featured by the weaker chemical activity compared with Portland cement, which hinders their wide application in solidification treatment.

Compressibilty is a crucial index to determine whether cement-treated dredged clay meets engineering requirement, especially for long-term soil settlement (Paul and Hussain, 2020, Shi *et al.* 2020, Shi *et al.* 2021b). There exist some studies with the emphasis on the deformation characteristic of reconstituted dredged clay (Hong *et al.* 2010, Zeng *et al.* 2016, Shahriar and Jadid 2018). The undesirable mechanical properties of raw dredged clay make it undergo the large deformation with time, which might cause some engineering problems for a foundation soil layer. The cement agent effectively improves the mechanical behavior of dredged clay through continuous hydration reactions and pozzolanic reactions. It is well recognized that cement treated dredged clay has the similar compression behavior to the natural deposited soil because of artificial structure (Jongpradist *et al.* 2010, Huang *et al.* 2011, Ali *et al.* 2020). Evaluation of artificial structure of cement-treated clay has been reported based on intrinsic compression concept (Burland 1990, Liu *et al.* 1999, Du *et al.* 2014, Bian *et al.* 2016).

However, it is still unclear how internal and external factors, especially pore fluid salinity affect compressibility of cement-treated marine dredged clay in the whole loading

*Corresponding author, Ph.D. Student
E-mail: wanxing1994@seu.edu.cn
[a]Associate Professor
E-mail: jwding@seu.edu.cn

ISSN: 2005-307X (Print), 2092-6219 (Online)

Fig. 1 Plane diagram of Dalian bay cross-sea traffic project

process. This research is carried out to guide a cross-sea traffic project in Dalian Bay, where marine dredged clay is proposed as filling materials of artificial islands after cement solidification treatment. A series of oedometer tests are performed to study the effect of cement addition on compressibility. The aim of the research includes: (1) to investigate how various factors affect compression behavior at both pre-yield and post-yield stage; (2) to discuss the effect of pore fluid salinity on reconstituted and cement-treated marine dredged clay; (3) to provide a practical method to evaluate compressibility of cement-treated dredged clay in practice.

2. Project overview

As shown in Fig. 1, the proposed sea-crossing traffic project is located in Dalian, Liaoning province, China, aiming to connect the downtown district to Jinpu new district. The whole project is about 25km long, composed of cross-sea bridges, under-sea tunnels and exchange artificial islands.

Note that a large volume of dredged clay (about 20 million cubic meters) would be generated in this project, including 10 million cubic meters from preliminary channel expansion, and the other 10 million cubic meters from excavation of the foundation of artificial islands. It is troublesome to deal with these dredged clays due to its extremely high water content and low strength. On the other hand, the construction of artificial islands requires a large volume of filling materials. Conventional methods such as quarrying, not only result in irreversible harm to surrounding environment, but also increases costs sharply in long-distance transportation. To this end, cement treated dredged clay is suggested as filling materials of artificial islands, which provides solution to both stockpiles of generated dredged clay and lack of construction materials. This treatment method is not only economical but also environmentally friendly.

Reasonable evaluation of deformation characteristics of cemented dredged clay is crucial for the design and construction of artificial islands, to achieve balance in safety and costs. Thus, a series of one-dimensional compression tests were carried out to provide reference for field application, followed by development of a practical method to predict compressibility of cemented clay.

3. Materials and experimental procedure

3.1 Materials

As shown in Fig. 2, dredged clay used in this study was sampled from the seabed of Dalian Bay. Table 1 shows basic physical properties of investigated marine dredged clay. It is seen that the clay is characterized by high water content of 71.6%, being higher than the liquid limit. The additive used in this study is ordinary Portland cement, PC 42.5, produced from a local cement manufacturer. The chemical compositions of Portland cement are shown in Table 2.

Table 1 Basic physical properties of investigated marine dredged clay

Property	Value
Water content / %	71.6
Liquid limit / %	53.1
Plastic limit / %	28.1
Specific gravity	2.70
Pore fluid salinity (g/L)	35.4
PH of pore fluid	7.99
Sand（0.075~2mm）/ %	4.0
Silt（0.005~0.075 mm）/ %	56.0
Clay（<0.005 mm）/ %	40.0

Fig. 2 Marine dredged clay after mixing

Table 2 Chemical composition of ordinary Portland cement

Compound	CaO	SiO_2	Al_2O_3	Fe_2O_3	SO_3	MgO	K_2O
%	62.33	20.98	4.29	2.07	2.84	1.90	1.01

Fig. 3 Desalination treatment of marine dredged clay by centrifugation

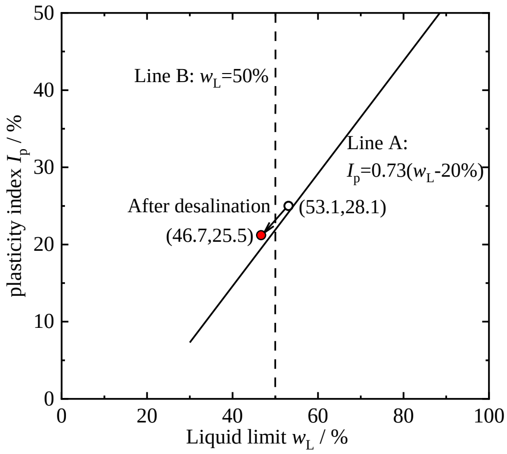

Fig. 4 Plasticity chart of dredged clay with and without pore salt

It should be noted that conventional calculation methods of water content may not be suitable herein, considering the fact that the pore salt in marine dredged clay would also transform to solids by oven-drying methods. The additional solids transformed from pore salt would result in errors in determination of water content (Noorany, 1984, ASTM D4542-15 2015). As shown in Eq. (1), the concept of fluid content proposed by Noorany (1984) is adopted in this paper, where m_s denotes the mass of soil particles, m_f denotes the mass of pore fluid. And the weight of pore fluid can be expressed as the sum of the mass of salt dissolved in the pore water m_{sa} and the mass of pore water m_w, as shown in Eq. (2).

$$w_f = \frac{m_f}{m_s} \times 100 \tag{1}$$

$$m_f = m_w + m_{sa} \tag{2}$$

To study the effect of pore fluid salinity on mechanical behavior of cemented marine dredged clay, treatment of desalination was performed on reconstituted dredged clay. The clay was first mixed with distilled water, and the pore fluid was then extracted from the clay with centrifugation, as shown in Fig.3. The stages were repeated for about three to four times until the pore fluid salinity was less than 2g/L. It can be seen in Fig. 4, with the decrease of pore fluid salinity from 35.4g/L to 1.2g/L, liquid limit w_L decreases obviously from 53.1 to 46.7, but plastic limit w_p changes relatively gently, which is consistent with the conclusions drawn by Song *et al.* (2017). It is noticed that the liquid limit of marine dredged clay decreases after treatment of desalination, attributed to the growing particle flocculation for non-expansive soils (Geertsema *et al.*2005, Ying *et al.* 2020).

3.2 Experimental procedure

Note that dredged clay is usually characterized by high water content being larger than its liquid limit. The water content is as high as 2~3 times of liquid limit especially for cutter suction dredger construction. Thus, initial water contents ranging from 1~3 times of liquid limit were adopted, including 58.2%, 80.0%, 107.6%, 135.8%, 164.6%. For comparison, the dredged clay after desalination treatment was also tested, with an initial water content of 103.9%. To prepare specimens, a predetermined quantity of water was first added to the dredged clay and then mixed to obtain five levels of initial water content. Afterwards, three levels of cement content (40, 80, 120 kg/m^3, by volume of wet clay) was poured into the clay-slurry and mixed for five to ten minutes to achieve uniformity.

To prepare oedometer test specimens, the mixture was then filled into a plastic cup by three steps, and the bubble in the mixture was eliminated by vibration constantly. The cutting ring was pressed into the soil mixture slightly after the filling height in the plastic cup exceeded 4cm. Slight vibration was conducted to guarantee sufficient contact of soil mixtures with inside surface of the cutting ring. As shown in Fig.5 (a), plastic cups along with the cutting rings were finally wrapped by sealing bags. The specimens for unconfined compressive strength tests were prepared by pushing materials into a cylindrical mold (with 39.1mm in diameter and 80mm in height). The specimens were all put into a curing room (20±2℃ temperature and 95% humidity). They were taken out after three curing period, including 7d, 28d and 60d. To carry out oedometer tests, plastic cups were cut and the contained soil mixture was trimmed, as shown in Fig. 5(b). The applied loading stress was started from 6.25 kPa. The following incremental loads were 12.5 kPa, 25 kPa, 50 kPa, 100 kPa, 200 kPa, 400 kPa, 800 kPa and 1600 kPa. To prevent remarkable change of mechanical behavior of specimens during testing process, each incremental loading was kept for only one hour. This method has been proved acceptable, considering the fact that over 90% consolidation degree of the specimen can be achieved (Wang and Abriak, 2015, Bian *et al.* 2016). The Unconfined compressive strength tests were performed following the methods of ASTM (2013). The mixing design and conducted experimental tests are summarized in Table 3.

Table 3 Mix design and tests performed in the experimental program

Classification	Sample number	Water content w (%)	Cement content A (kg/m^3)	Salinity S_{PL} (g/L)	Curing time T (d)	Oedometer tests	UCS tests
Remolded clay	W1	58.2	--	35.4	--	✓	×
	W2	80.0	--	35.4	--	✓	×
Remolded clay with desalination treatment	XW1	56.2	--	1.2	--	✓	×
	XW2	77.2	--	1.2	--	✓	×
Cemented clay	W1C1	58.2	40	35.4	7/28/60	×	✓
	W1C2	58.2	80	35.4	7/28/60	✓	✓
	W1C3	58.2	120	35.4	7/28/60	×	✓
	W2C1	80.0	40	35.4	7/28/60	×	✓
	W2C2	80.0	80	35.4	7/28/60	✓	✓
	W2C3	80.0	120	35.4	7/28/60	×	✓
	W3C1	107.6	40	35.4	7/28/60	✓	✓
	W3C2	107.6	80	35.4	7/28/60	✓	✓
	W3C3	107.6	120	35.4	7/28/60	✓	✓
	W4C1	135.8	40	35.4	7/28/60	×	✓
	W4C2	135.8	80	35.4	7/28/60	✓	✓
	W4C3	135.8	120	35.4	7/28/60	×	✓
	W5C1	164.6	40	35.4	7/28/60	×	✓
	W5C2	164.6	80	35.4	7/28/60	✓	✓
	W5C3	164.6	120	35.4	7/28/60	×	✓
Cemented clay with desalination treatment	XW3C1	103.9	40	1.2	7/28/60	✓	✓
	XW3C2	103.9	80	1.2	7/28/60	✓	✓
	XW3C3	103.9	120	1.2	7/28/60	✓	✓

"✓" denotes the test was conducted, "×" denotes the test was not conducted

(a) Plastic cups containing treated dredged clay

(b) Handling of a single specimen

Fig. 5 Preparation of specimens for oedometer tests

Oedometer tests were also conducted on reconstituted clay at initial water content of 58.2% and 80.0% with and without pore salt, not only to explore pore fluid salinity effect on reconstituted clay but also provide a reference for evaluating soil structure of cement-treated clay. The reconstituted soils with targeted initial water content were carefully put into the oedometer rings by controlling the mass of the specimen, which can be calculated in a fully saturated condition. It should be mentioned that the error between measured specimen mass and calculated mass should be within 3.6 g (Song *et al.* 2017).

Due to very low stiffness of reconstituted clay specimens, the problem of soil squeezing out through the clearance gap between the ring and the upper porous disc should be addressed. Hong *et al.* (2010) recommended that the modified oedometer apparatus starting from a very low effective vertical stress of 0.5 kPa can be used to avoid the problems of squeezing out. Thus, the oedometer tests in this study were carried out following Hong *et al.* (2010). The specimens of reconstituted clay had a diameter of 61.8 mm and a height of 40 mm. The duration of each incremental load was about 3 days, following the methods presented by Zeng *et al.* (2011).

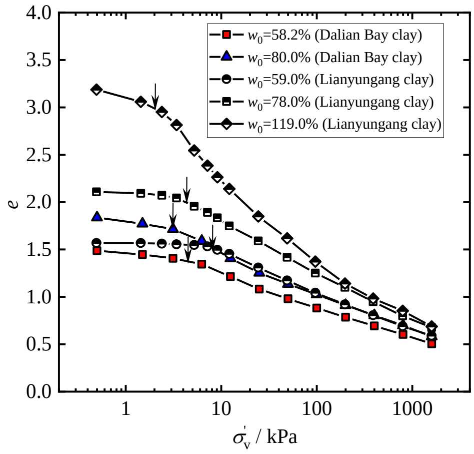

Fig. 6 Compression curves of reconstituted clay at various initial water content

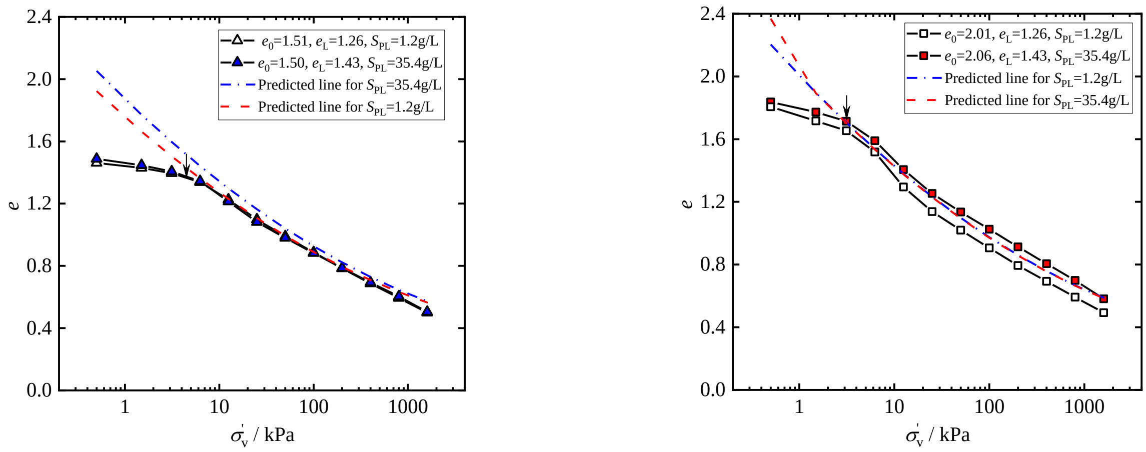

(a) w_0 =58.2%, 56.2% (b) w_0 =80.0%, 77.2%

Fig. 7 Compression curves of reconstituted dredged clay with and without pore salt

4. Results and discussion

4.1 Compression behavior of reconstituted clay

As shown in Fig. 6, compression curve of reconstituted marine dredged clay shows an inverse "S" shape due to suction pressure, where the yielding point is referred to remolded yield stress by Hong *et al.* (2010). Similar to soft natural soils, the compression index of reconstituted clay increases dramatically after remolded yield stress. The remolded yield stress of remolded clay at initial water content of 58.2% and 80.0% is 5.3 kPa and 3.2 kPa respectively by methods of ln(1+e)-logσ (Butterfield 1979). Compression curves of reconstituted Lianyungang clay are also introduced for comparison (Hong *et al.* 2010). In terms of a specific reconstituted clay, the remolded yield stress decreases with increasing initial water content. Furthermore, the Lianyungang clay has a higher remolded yield stress than Dalian Bay clay with a certain initial water content. The difference of void ratio e_L at liquid limit is considered mainly responsible for the different suction pressure.

Fig. 7 depicts the influence of pore fluid salinity on compression behavior of reconstituted marine dredged clay. It is noted that the difference is negligible between reconstituted clay with and without pore salt at about 58.2% initial water content. However, when the initial water content reaches 80.0%, the compression curve of clay containing pore salt lies above the other obviously. The difference of void ratio between two lines increases with loading stress. It is inferred the pore salt plays positive role in resisting deformation. The change of compression behavior with pore fluid salinity has been well correlated with liquid limit (Song *et al.* 2017). As discussed previously in Fig. 4, the liquid limit of marine dredged clay decreases after desalination treatment, resulting in a decrease of void ratio at liquid limit. Therefore, the compressibility of reconstituted clay increases after desalination treatment (Hong *et al.* 2010).

To assess effect of cement addition on compressibility, accurate compression curves of raw reconstituted dredged clay are needed. Due to limited experimental data of reconstituted clay, extended intrinsic compression line (EICL) proposed by Hong *et al.* (2010) is adopted herein to act as a baseline for evaluating artificial structure of cemented clay. The EICL was developed from the ICL presented by Burland (1990). The application scope of initial water content was extended from 1.0~1.5 times liquid limit to 0.7~2.0 times liquid limit. The expression of EICL is presented as Eq. (3). Note that the parameters of C^*_c and

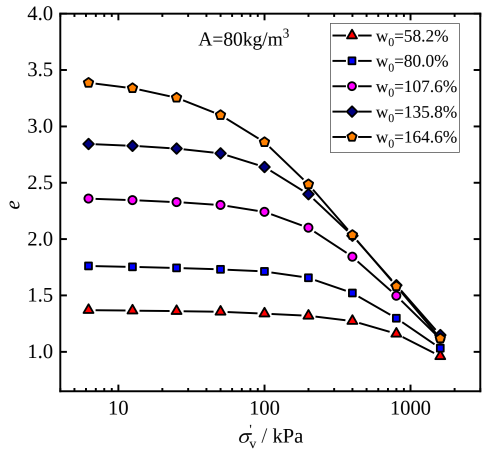

Fig. 8 Compression curves of cement-treated dredged clay at various initial water content after 7 days curing

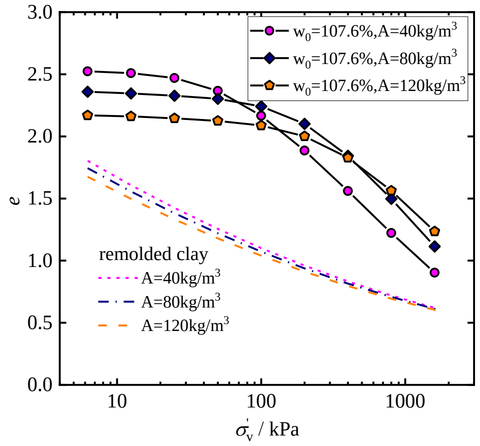

Fig. 9 Compression curves of cement-treated dredged clay with different cement content after 7 days curing

e^*_{100} need to be determined to assess the intrinsic compression line. It is suggested that C^*_c and e^*_{100} can be related to initial void ratio e_0 and void ratio at liquid limit e_L (Zeng *et al.* 2015), which is shown as Eqs. (4) and (5).

$$e^* = [3.0 - 1.87\log\sigma'_v + 0.179(\log\sigma'_v)^2] \times C^*_c + e^*_{100} \quad (3)$$

$$e^*_{100} = 0.357 + 0.171e_0 + 0.223e_L \quad (4)$$

$$C^*_c = -0.069 + 0.109e_0 + 0.152e_L \quad (5)$$

The predicted compression lines of reconstituted dredged clay with and without pore salt are presented in Fig. 7. Good fitness can be observed between predicted and measured curves beyond remoulded yield stress. It is evident that EICL can be adopted as a baseline of cement-treated clay. Considering the fact that oedometer tests of cement-treated clay started from 6.25 kPa, the discrepancy between predicted and measured value within remoulded yield stress can be ignored.

4.2 Compression behavior of cement-treated clay

Fig. 8 shows the compression curves of cement-treated clay at various initial water content ranging from 58.2% to 164.6% after 7 days curing, where the cement addition is a constant value of 80 kg/m^3. It can be seen that the compression curves of cemented clay at various initial state show similar evolution law during loading process. The compression index is low within the yield stress, after which the compressibility increases dramatically, demonstrating the degradation of soil structure (Hong *et al.* 2010, Shi *et al.* 2021a). To note that the specimens at higher initial water content show higher after-curing void ratio but lower yield stress due to weaker cementation bonding effect. However, the compression behavior is dominated by the fabric of the cemented clay and the applied loading stress beyond yield stress. The compression curves tend to converge the same line with increasing loading stress (Kamruzzaman *et al.* 2009, Sasanian *et al.* 2014). It can be concluded that the initial water content of dredged clay plays a dominant role during pre-yield stage by controlling after-curing void ratio and the yield stress. In contrast, the effect of initial water content is negligible during post-yield stage.

Fig. 9 shows compression curves of cemented clay with different cement content. The reference lines of destructed clay (Eq. (3)) are also presented, which varies with cement content due to the differences in after-curing void ratio. It can be observed that the cement content generates a persistent effect on the compression behavior during whole loading process. The compression curves of cemented clay with various cement content do not converge even at high loading stress. Considering the fact that the cement hydration and pozzolanic reactions consume water with production materials as solid content during curing time (Horpibulsuk *et al.* 2005, Ding *et al.* 2019a), the specimens with higher cement content are featured with smaller after-curing void ratio. Moreover, higher cement content results in stronger cementitious bonds, leading to higher yield stress but slower destruction rate at post-yield stage.

Fig. 10 reflects the effect of curing time on the compressibility of cement-treated clay. The curing period has negligible effect on the after-curing void ratio, and the curves are almost overlapped at pre-yield stage. It can be noticed that the compressibility of cement-treated clay after longer curing time is obviously lower at post-yield stage, which can be attributed to stronger cementitious bonds due to more sufficient cement hydration and pozzolanic reactions. The degradation of artificial structure is rather fast for specimens after 7 days curing time. However, as the curing time reaches 28 days, the cement-treated clay shows stronger ability to maintain artificial structure at post-yield stage. Moreover, it is found that the effect of curing time relies on the initial water content. As shown in Fig. 10 (a), with lower initial water content, the compressibility of the specimen remains almost unchanged as the curing time increases from 28 days to 60 days. In contrast, with much higher water content [Fig. 8(b)], the effect of the curing time is predominant even after 28 days, which can be ascribed to inadequate chemical reactions at early stages.

Fig. 11 reflects the effect of pore fluid salinity on compression and strength behavior of cemented clay. It can be observed that the pore salt has negative effect on compression behavior of cemented clay, especially at post-

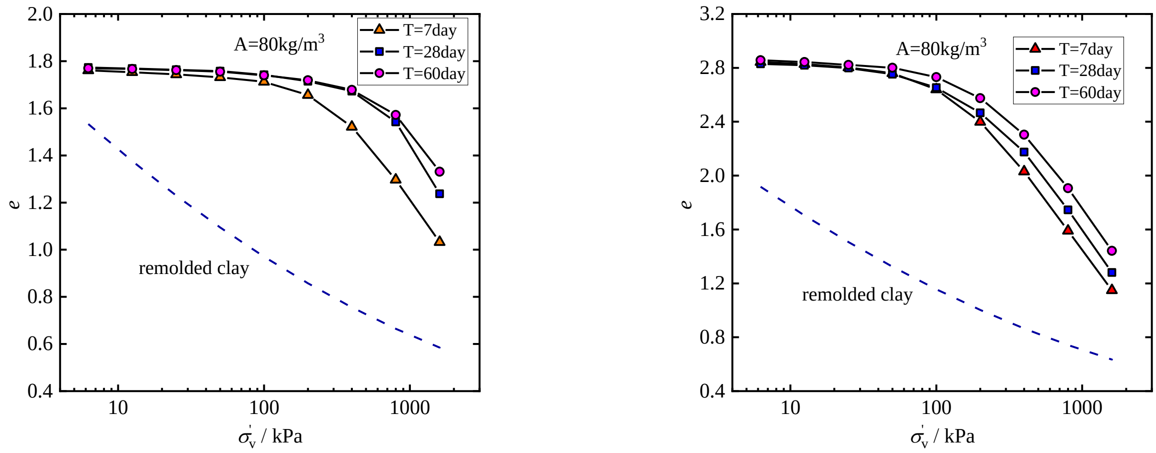

(a) w_0 =80.0% (b) w_0 =135.8%

Fig. 10 Compression curves of cement-treated dredged clay at different curing time

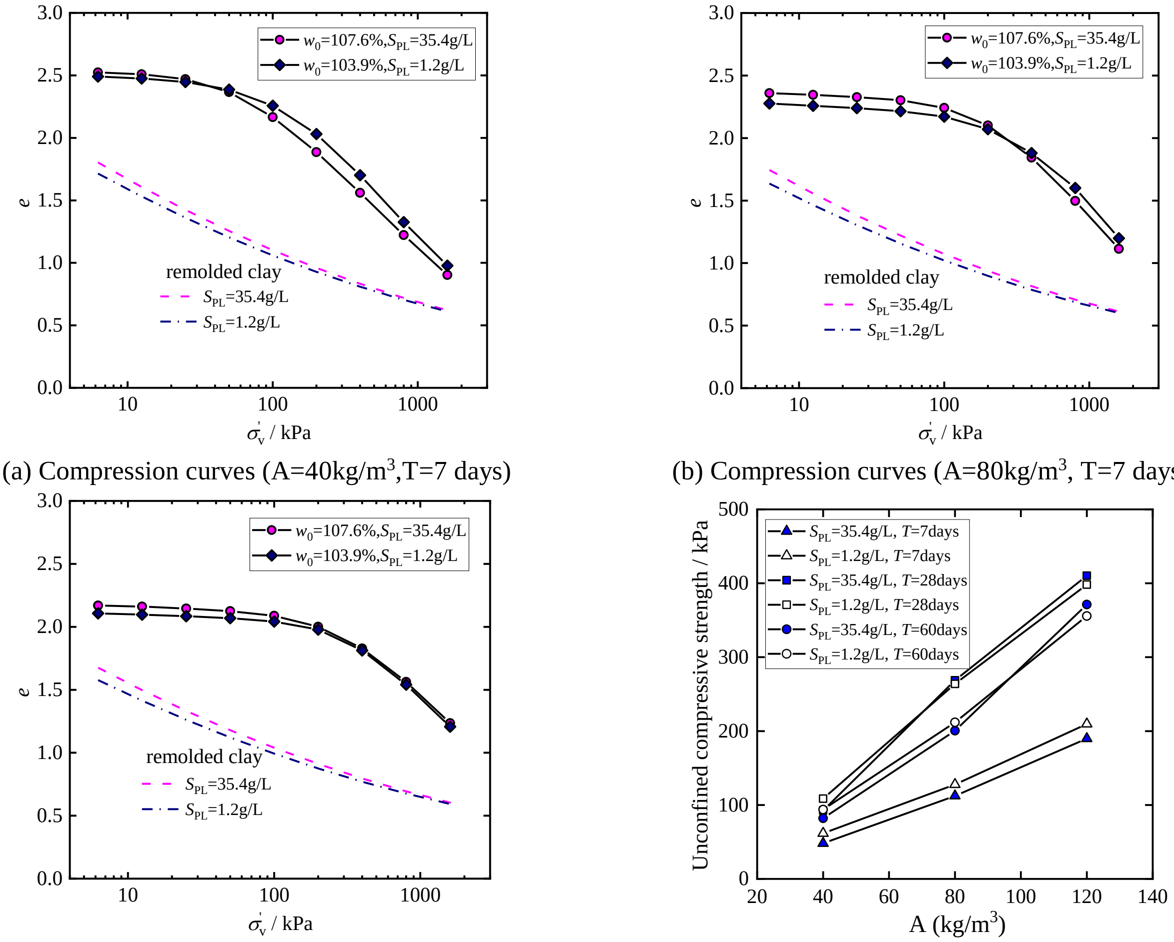

(a) Compression curves (A=40kg/m^3,T=7 days) (b) Compression curves (A=80kg/m^3, T=7 days)

(c) Compression curves (A=120kg/m^3, T=60 days) (d) Unconfined compressive strength

Fig. 11 Effect of pore salt on the compression and strength behavior of cement-treated dredged clay

yield stage. The chemical reaction between chloride ions and calcium aluminate may be responsible for the negative effect, considering the produced calcium chloroaluminate hydrate shows worse mechanical behavior than hydrate calcium silicate (Ahsan *et al.* 2020, Sara *et al.* 2020). Moreover, it is obvious to note that the effect of pore fluid salinity relies on the cement content and curing time significantly. With low cement content of 40 kg/m^3 after 7 days curing, the compressibility of specimens with and without pore salt is almost the same within yield stress, but the degradation of artificial structure of specimens with pore salt is obviously faster at post-yield stage. As cement content and curing time increases, the impact of pore fluid salinity fades. When the cement content is as high as 120 kg/m^3 after 60 days curing, compression curves are almost overlapped. It is inferred that with increasing cement content and curing time, the negative effect of chloridion is decreased by crystallization and expansion effects of solute salts (Zhang *et al.* 2013). As shown in Fig.11(d), the variation of unconfined compressive strength shows similar evolution. The effect of pore salt even becomes positive with high cement content and long curing time.

5. Assessment of compression curves

Note that oedometer test is regarded time-consuming, which restrict the efficient evaluation of compressibility of cement-treated dredged clay with various water content, pore fluid salinity, cement content and curing time. Thus, a simple method is needed to predict compressibility of treated dredged clay in Dalian Bay.

It has been widely reported that cement-treated dredged clay shows similar evolution to natural structured soils in compression behavior. The compression curve is predominantly divided by the point of yield stress, that is to say the compressibility is totally different before and after the breakup of the soil structure (Liu and Cater. 1999, Du *et al.* 2014, Mujtaba *et al.* 2020). As shown in Fig. 12, the additional void ratio Δe demonstrates the soil structure of

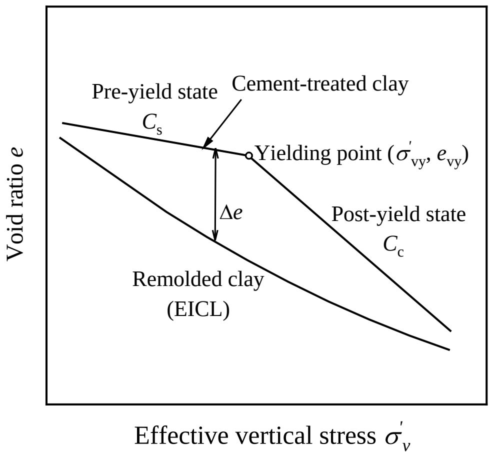

Fig. 12 Typical Compression curve of cement-treated dredged clay

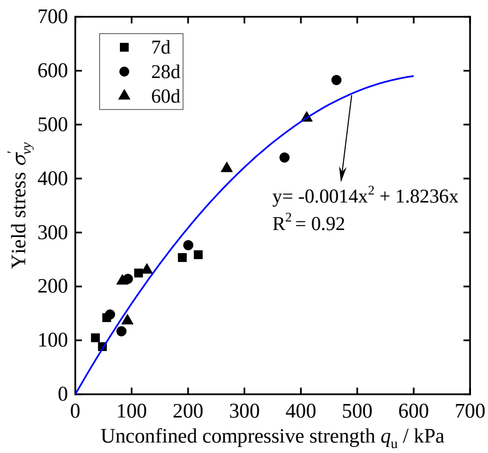

Fig. 13 Relationship between yield stress and unconfined compressive strength

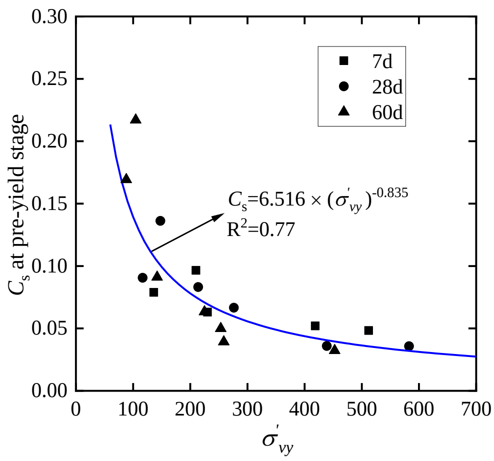

Fig. 14 Relationship between compression index at pre-yield state and yield stress

cemented clay compared with remolded clay. It can be seen that the compression index C_s is rather small at the pre-yield state, but the compression index increases sharply after the yielding point, indicating fast degradation speed of artificial structure.

As mentioned above, it is reasonable to deal with the compression line of cemented clay in pre-yield stage and post-yield stage respectively. To this end, the first objective is to obtain the yielding point of the compression curve. Considering the yield stress of cemented clay reflects the magnitude of the cementation, it is rational to correlate the magnitude of the yield stress with the strength characteristics (Du *et al.* 2013, Horpibulsuk *et al.* 2013, Bian *et al.* 2016). The experimental results of specimens (including number of W1C1, W2C2, W3C3, W4C4, W5C5) at three levels of curing time are used. Fig. 13 presents the relationship between yield stress and unconfined compressive strength of cemented-treated Dalian clay. It is found that the yield stress increases with unconfined compressive strength with an approximately square relation, as shown in Eq. (6). Thus, the yielding point can be easily obtained after the conduction of unconfined compressive tests.

$$\sigma'_{vy} = -0.0014 \times q_u^2 + 1.8236 \times q_u \tag{6}$$

To describe the compression curve at pre-yield stage, it can be considered a straight line with acceptable error, that is to say the compression line can be drawn after the determination of the after-curing void ratio and the compression index C_s. As shown in Fig. 14, it is found that C_s can be determined by yield stress by Eq. (7) with fitting coefficients of 0.77. Due to rather low compressibility of cemented clay at pre-yield stage, it is acceptable to draw the compression line before yielding point according to Eq. (8).

$$C_s = 6.516 \times (\sigma'_{vy})^{-0.835} \tag{7}$$

$$e = e_0 - C_s \times \log \sigma'_v \tag{8}$$

Regarding the compression line in post-yield stage, the artificial cemented dredged clay show similar mechanical

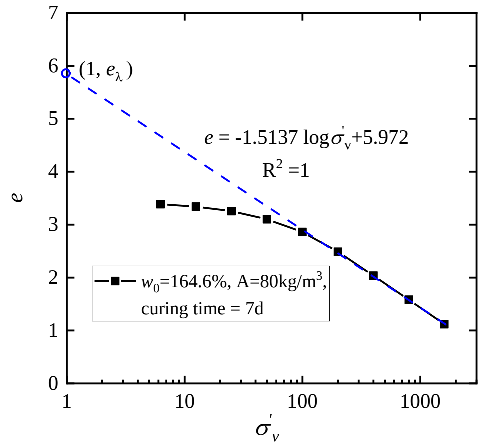

Fig. 15 Fitting line of compression behavior of cemented clay at post-yield stage

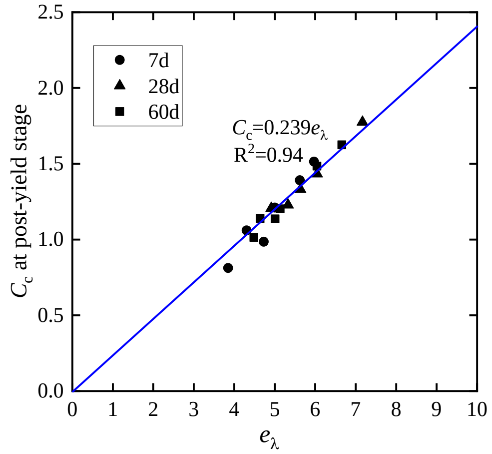

Fig. 16 Relationship between compression index at post-yield state and void ratio at 1 kPa stress

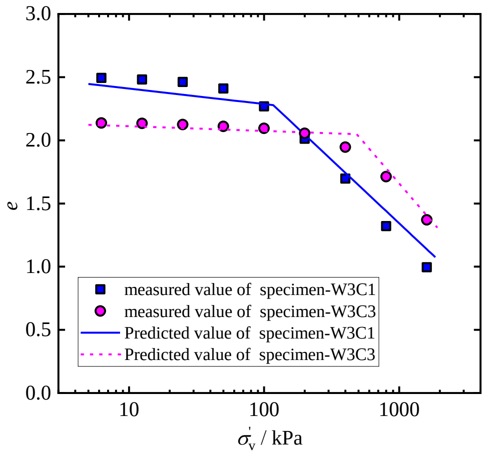

Fig. 17 Comparison of predicted and measured line of compression curves of cement-treated dredged clay

behavior to the reconstituted clay due to the breakage of the bonds. Thus, as shown in Eq. (9), predicting methods for compression behavior of reconstituted soils can be adopted (Burland 1990, Nagaraj *et al.* 1994), where e_n denotes a normalized void ratio, and a and b are normalized parameters which can be obtained through experiments. For better understanding, Eq. (9) can be rewritten as Eq. (10), here b/a just represents an experimental parameter.

$$\frac{e}{e_n} = a - b \times \log \sigma'_v \tag{9}$$

$$\frac{e}{a \times e_n} = 1 - \frac{b}{a} \times \log \sigma'_v \tag{10}$$

As shown in Fig. 15, the e_λ (the void ratio at σ'_v=1 kPa), a pressure based, normalizing reference volume, is used here following Sasanian and Newson (2014). To note in Fig. 13, the compression behavior of cemented clay at post-yield stage can be perfectly simulated through Eq. (11), which can be easily derived to Eq. (12). To compare the form of Eq. (10) with that of Eq. (12), it is easy to notice the C_c/e_λ plays the same role as b/a in the function. Thus, it can be inferred that C_c and e_λ can be correlated with an approximately linear relationship.

$$e = e_\lambda - C_c \times \log \sigma'_v \tag{11}$$

$$\frac{e}{e_\lambda} = 1 - \frac{C_c}{e_\lambda} \times \log \sigma'_v \tag{12}$$

For verifying, Fig. 16 presents the data of the parameter of C_c and e_λ obtained in this study. The results show that linear relationship exactly exists between C_c and e_λ with fitting coefficients of 0.94 (Eq. (13)). Thus, the compression line at post-yield stress can be formulated with only one unknown parameter e_λ (Eq. (14)), and this value can be determined easily by substituting the yield stress σ'_{vy} and corresponding void ratio e_{vy}.

$$C_c = 0.239 \times e_\lambda \tag{13}$$

$$\frac{e}{e_\lambda} = 0.9119 - 0.2102 \log \sigma'_v \tag{14}$$

To sum up, the rational compression curve of cement-treated dredged clay in Dalian can be evaluated by the following stages:

(1) Do unconfined compression test, determine the value of after-curing void ratio e_0 and unconfined compressive strength q_u

(2) Calculate consolidated yield stress σ'_{vy} through q_u using Eq. (6).

(3) Calculate C_s at pre-yield stage using Eq. (7), draw the pre-yield state compression curve using Eq. (8).

(4) determine e_λ by substituting yield stress σ'_{vy} and corresponding void ratio e_{vy}.

(5) draw the post-yield state compression curve using Eq. (14).

To validate the feasibility of the proposed prediction methods, experimental results of specimens of number "W3C1 and W3C3" are compared with predicted value. As shown in Fig. 17, general coincide can be observed between the testing and calculation results. The discrepancy seems larger under low vertical stress as for specimen-W3C1. The reasons may be attributed to the weaker artificial structure of cement-treated dredged clay with lower cement content. Overall, the proposed method can well reflect the evolution law of void ratio with loading stress with acceptable error. Rational compression curves can be obtained immediately after the determination of after-curing void ratio and unconfined compressive strength.

6. Conclusions

Cement-treated marine dredged clay is proposed as filling materials for the construction of artificial islands in Dalian Bay, China. To evaluate influence of cement addition on compressibility, a series of oedometer tests were carried out on original dredged clay and cement-treated clay. The effects of initial water content, cement content and curing time were investigated. The pore fluid salinity effect on compressibility of reconstituted and cement-treated clay was examined. Moreover, a practical method was presented to help quickly capture the compression curve in practice. The main conclusions are as following:

- The vertical yield stress of cemented clay decreases significantly with increasing initial water content of dredged clay due to weak cementitious bonds, but the compression lines tend to converge at high loading stress.
- The cement content dominates the degradation speed beyond the yielding point, the lower content of cement addition leads to smaller yield stress and faster degradation speed.
- The effect of pore fluid salinity on the reconstituted clay and cemented clay is totally different. It increases capacity of reconstituted dredged clay in resisting deformation by increasing liquid limit. In contrast, it predominantly accelerates the degradation speed of artificial structure after yielding point in cemented clay due to chemical reactions.
- A practical method is presented to estimate the compressibility of cement-treated clay in Dalian Bay. The compression lines can be easily determined after the determination of the after-curing void ratio and the unconfined compressive strength, and the predicted value generally agrees with the experimental data.

Acknowledgments

This study is partially supported by the National Natural Science Foundation of China (Grant No. 51978159) and National Key R&D Program of China (Grant No. 2015BAB07B06). The authors are grateful to Mr. Bobo Zhan for his hard work in the laboratory tests, which are essential to the successful completion of this manuscript.

References

Ali, M., Aziz, M., Hamza, M. and Madni, M.F. (2020), “Engineering properties of expansive soil treated with polypropylene fibers”, *Geomech. Eng.*, **22**(3), 227-236. https://doi.org/10.12989/gae.2020.22.3.227.

Ahsan, M.K., Barman, D.C., Shaikh, M. and Maqsood, Z. (2020), “Influence of salinity exposure on the mechanical properties of cement-treated sand”, *Geotech. Res.*, **7**(3), 161-172. https://doi.org/10.1680/jgere.20.00013.

Arefnia, A., Dehghanbanadaki, A., Kassim, K.A. and Ahmad, K. (2020), “Stabilization of backfill using TDA material under a footing close to retaining wall”, *Geomech. Eng.*, **22**(3), 197-206. https://doi.org/10.12989/gae.2020.22.3.197.

ASTM D2166-13 (2013), Standard Test Method for Unconfined Compressive Strength of Cohesive Soil. American Society for Testing and Materials, West Conshohocken, Pennsylvania, U.S.A.

ASTM D4542-15 (2015), Standard Test Methods for Pore Water Extraction and Determination of the Soluble Salt Content of Soil by Refractometer.” American Society for Testing and Materials, West Conshohocken, Pennsylvania, U.S.A.

Bian, X., Wang, Z.F., Ding, G.Q. and Cao, Y.P. (2016), “Compressibility of cemented dredged clay at high water content with super-absorbent polymer”, *Eng. Geol.*, **208**, 198-205. https://doi.org/10.1016/j.enggeo.2016.04.036.

Burland, J.B. (1990), “On the compressibility and shear strength of natural soils”, *Géotechnique*, **40**(3), 329-378. https://doi.org/10.1680/geot.1990.40.3.329.

Çevikbilen, G., Basar, H.M., Karadogan, Ü., Teymur, B., Daglı, S. and Tolun, L. (2020), “Assessment of the use of dredged marine materials in sanitary landfills: A case study from the Marmara sea”, *Waste Manage.*, **113**, 70-79. https://doi.org/10.1016/j.wasman.2020.05.044.

Butterfield, R. (1979), “A natural compression law for soils”, *Géotechnique*, **29**(4), 469-480. https://doi.org/10.1680/geot.1979.29.4.469.

Ding, J.W., Feng, X.S., Xu, G.Z., Qian, S. and Ji, F. (2019a), “Strength properties and microstructural characteristics of stabilized dredged materials at high water contents”, *J. Test. Eval.*, **47**(3), 2225-2239. https://doi.org/10.1520/JTE20180049.

Ding, J.W., Shi, M.L., Liu, W.Z. and Wan, X. (2019b), “Failure of roadway subbase induced by overuse of phosphogypsum”, *J. Perform. Constr. Fac.*, **33**(2), 04019013. https://doi.org/10.1061/(ASCE)CF.1943-5509.0001278.

Du, Y.J., Horpibulsuk, S., Wei, M.L., Suksiripattanapong, C. and Liu, M.D. (2014), “Modelling compression behavior of cement-treated zinc-contaminated clayed soils”, *Soils Found.*, **54**(5), 1018-1026. https://doi.org/10.1016/j.sandf.2014.09.007.

Geertsema, M. and Torrance, J.K. (2005), “Quick clay from the Mink Creek landslide near Terrace, British Columbia: Geotechnical properties, mineralogy, and geochemistry”, *Can. Geotech. J.*, **42**(3), 907-918. https://doi.org/10.1139/t05-028.

Hong, Z.S., Yin, J. and Cui, Y.J. (2010), “Compression behaviour of reconstituted soils at high initial water contents”, *Géotechnique*, **60**(9), 691-700. https://doi.org/10.1680/geot.09.P.059.

Horpibulsuk, S., Norihiko, M. and Nagaraj, T.S. (2005), “Clay-water/cement ratio identity for cement admixed soft clays”, *J. Geotech. Geoenviron. Eng.*, **131**(2), 187-192. https://doi.org/10.1061/(ASCE)1090-0241(2005)131:2(187).

Horpibulsuk, S., Rachan, R., Suddeepong, A., Liu, M.D. and Du, Y.J. (2013), “Compressibility of lightweight cemented clays”, *Eng. Geol.*, **159**, 59-66. https://doi.org/10.1016/j.enggeo.2013.03.020.

Huang, Y.H., Zhu, W., Qian, X.D., Zhang, N. and Zhou, X.Z. (2011), “Change of mechanical behavior between solidified and remolded solidified dredged materials”, *Eng. Geol.*, **119**(3-4), 112-119. https://doi.org/10.1016/j.enggeo.2011.03.005.

Jongpradist, P., Youwai, S. and Jaturapitakkul, C. (2010), “Effective void ratio for assessing the mechanical properties of

cement-clay admixtures at high water content", *J. Geotech. Geoenviron. Eng.*, **137**(6), 621-627. https://doi.org/10.1061/(ASCE)GT.1943-5606.0000462.
Kamruzzaman, A.H., Chew, S.H. and Lee, F.H. (2009), "Structuration and destructuration behavior of cement-treated Singapore marine clay", *J. Geotech. Geoenviron. Eng.*, **135**(4), 573-589. https://doi.org/10.1061/(ASCE)1090-0241(2009)135:4(573).
Kim, H.J., Won, M.S., Lee, J.B., Joo, J.H. and Jamin, J.C.(2015), "Comparative study on the behavior of soil fills on rigid acrylic and flexible geotextile containers", *Geomech. Eng.*, **9**(2), 243-259. https://doi.org/10.12989/gae.2015.9.2.243.
Liu, M.D. and Carter, J.P. (1999). "Virgin compression of structured soils", *Géotechnique*, **49**(1), 43-57. https://doi.org/10.1680/geot.1999.49.1.43.
Mujtaba, H., Khalid, U., Farooq, K., Elahi, M., Rehman, Z. and Shahzad, H.M. (2020), "Sustainable utilization of powdered glass to improve the mechanical behavior of fat clay", *KSCE J. Civ. Eng.*, **24**(12), 3628-3639. https://doi.org/10.1007/s12205-020-0159-2.
Mymrin, V., Scremim, C.B., Stella, J.C., Pan, R.C.Y., Avanci, M.A., Bosco, J.C. and Rolim, P. (2021), "Environmentally clean materials from contaminated marine dredged sludge, wood ashes and lime production wastes", *J. Clean. Prod.*, **307**, 127074. https://doi.org/10.1016/j.jclepro.2021.127074.
Nagaraj, T.S., Pandian, N.S. and Narasimha R.P.S.R. (1994). "Stress-state-permeability relations for overconsolidated clays", *Géotechnique*, **44**(2), 349-352. https://doi.org/10.1680/geot.1996.46.2.363
Noorany, I. (1984), "Phase relations in marine soils", *J. Geotech. Eng.*, **110**(4), 539-543. https://doi.org/10.1061/(ASCE)0733-9410(1984)110:4(539).
Paul, A. and Hussain, M. (2020), "An experiential investigation on the compressibility behavior of cement-treated Indian peat", *B. Eng. Geol. Environ.*, **79**(3), 1471-1485. https://doi.org/10.1007/s10064-019-01623-x.
Sara, G., Stefania, L., Barbara, l. and Alessandro, F. (2020), "Effect of the pore fluid salinities on the behaviour of an electrokinetic treated soft clayey soil", *Soils Found.*, **60**(4), 898-910. https://doi.org/10.1016/j.sandf.2020.06.003.
Sasanian, S. and Newson, T.A. (2014), "Basic parameters governing the behaviour of cement-treated clays", *Soils Found.*, **54**(2), 209-224. https://doi.org/10.1016/j.sandf.2014.02.011.
Shahriar, A.R. and Jadid, R. (2018), "An experimental investigation on the effect of thixotropic aging on primary and secondary compression of reconstituted dredged clays", *Appl. Clay Sci.*, **162**(15), 524-533. https://doi.org/10.1016/j.clay.2018.05.023.
Shi, X.S., Gao, Y.F., and Ding, J.W. (2021a), "Estimation of the compression behavior of sandy clay considering sand fraction effect based on equivalent void ratio concept", *Eng. Geol.*, **280**, 105930. https://doi.org/10.1016/j.enggeo.2020.105930.
Shi, X. S., Liu, K. and Yin, J.H. (2021b), "Effect of initial density, particle shape, and confining stress on the critical state behavior of weathered gap-graded granular soils", *J. Geotech. Geoenviron. Eng.*, **147**(2), 04020160. https://doi.org/10.1061/(ASCE)GT.1943-5606.0002449.
Shi, X.S. and Zhao, J.D. (2020), "Practical estimation of compression behavior of clayey/silty sands using equivalent void ratio concept", *J. Geotech. Geoenviron. Eng.*, **146**(6), 04020046. https://doi.org/10.1061/(ASCE)GT.1943-5606.0002267.
Slimanou, H., Eliche-Quesada, D., Kherbache, S., Bouzidi, N. and Tahakourt, A.K. (2020), "Harbor Dredged Sediment as raw material in fired clay brick production: Characterization and properties", *J. Build. Eng.*, **28**, 101085. https://doi.org/10.1016/j.jobe.2019.101085.
Song, M.M, Zeng, L.L. and Hong, Z.S. (2017), "Pore fluid salinity effects on physicochemical-compressive behaviour of reconstituted marine clays", *Appl. Clay Sci.*, **146**, 270-277. https://doi.org/10.1016/j.clay.2017.06.015.
Vafaei, D., Hassanli, R., Ma, X., Duan, J.M. and Yan, Z.G. (2021), "Sorptivity and mechanical properties of fiber-reinforced concrete made with seawater and dredged sea-sand", *Constr. Build. Mater.*, **270**, 121436. https://doi.org/10.1016/j.conbuildmat.2020.121436.
Wang, D. and Abriak, N.E. (2015), "Compressibility behavior of Dunkirk structured and reconstituted marine soils", *Mar. Georesour. Geotec.*, **33**(5), 419-428. https://doi.org/10.1080/1064119X.2014.950798.
Xu, G.Z., Feng, Z.Y., Yin, J. Han W.X., Ahmed, S. and Miao, Y.H. (2020), "Effect of salinity on rheological behavior of cement-treated dredged clays as fills", *J. Mater. Civ. Eng.*, **32**(9), 04020269. https://doi.org/10.1061/(ASCE)MT.1943-5533.0003376.
Yamashita, E., Cikmit, A.A., Tsuchida, T. and Hashimoto, R. (2020), "Strength estimation of cement-treated marine clay with wide ranges of sand and initial water contents", *Soils Found.*, **60**(5), 1065-1083. https://doi.org/10.1016/j.sandf.2020.05.002.
Ying, Z., Cui, Y.J. Duc, M., Benahmed, N., Bey, H.B. and Chen, B. (2021), "Salinity effect on the liquid limit of soils", *Acta Geotech.*, **16**(4), 1101-1111. https://doi.org/10.1007/s11440-020-01092-7.
Yoobanpot, N., Jamsawang, P., Krairan, K., Jongpradist, P. and Horpibulsuk, S. (2018), "Reuse of dredged sediments as pavement materials by cement kiln dust and lime treatment", *Geomech. Eng.*, **15**(4), 1005-1016. https://doi.org/10.12989/gae.2018.15.4.1005.
Zhang, C.L., Zhu, W., Li, L. and Fan, G.J. (2007), "Field test of dike construction with solidified lake dredged material", *China Harbour Eng.*, **147**(1), 27-29. https://doi.org/10.3969/j.issn.1003-3688.2007.01.008.
Zhang, D.W., Fan, L.B., Liu, S.Y. and Deng, Y.F. (2013), "Experimental investigation of unconfined compression strength and stiffness of cement treated salt-rich clay", *Mar. Georesour. Geotec.*, **31**(4), 360-374. https://doi.org/10.1080/1064119X.2012.690826.
Zeng, L.L., Hong, Z.S., Cai, Y.Q. and Han, J. (2011), "Change of hydraulic conductivity during compression of undisturbed and remolded clays", *Appl. Clay Sci.*, **51**(1), 86-93. https://doi.org/10.1016/j.clay.2010.11.005.
Zeng L.L., Hong Z.S. and Cui Y.J. (2015), "Determining the virgin compression lines of reconstituted clays at different initial water contents", *Can. Geotech. J.*, **52**(9), 1408-1415. https://doi.org/10.1139/cgj-2014-0172.
Zeng L.L., Hong Z.S. and Cui Y.J. (2016), "Time-dependent compression behaviour of dredged clays at high water contents in China", *Appl. Clay Sci.*, **123**, 320-328. https://doi.org/10.1016/j.clay.2016.01.039.

CC